Transverse Resonance Analysis of Finline Discontinuities

ROBERTO SORRENTINO, MEMBER, IEEE, AND TATSUO ITOH, FELLOW, IEEE

Abstract —**A method of analysis is proposed for characterizing finline discontinuities. Two conducting or magnetic planes are inserted at some distances away from the discontinuity so as to obtain a closed resonant structure. A transverse resonance technique is then used to compute the resonant frequencies and, from these, the equivalent circuit parameters of the discontinuity. In the particular case when the discontinuity is removed, the method can be used to characterize uniform finlines.**

I. Introduction

FINLINES are now recognized as a suitable technology of millimeter-wave integrated circuits. While much theoretical work has been done concerning the analysis and characterization of uniform finline structures [1], [2], a relatively small number of analyses of finline discontinuities have been developed [3], [4].

This paper presents a new method of analysis and characterization of both uniform finlines and finline discontinuities. The method consists of computing the resonant frequencies of a resonator obtained by inserting two conducting or magnetic planes apart from the discontinuity; using a transverse resonance technique, the electromagnetic (EM) fields are expanded in terms of longitudinal section magnetic (LSM) and electric (LSE) modes of the rectangular waveguide. With respect to other approaches based on the field expansion in terms of finline modes [3], [4], the present one has the advantage of a substantial reduction of computer time. In this paper, this new method is applied to the simple step discontinuity as well as to the cascade of step discontinuities.

II. Characterization of the Discontinuity

The characterization of a finline discontinuity is obtained with the resonant frequencies of resonators which are obtained by introducing two shorting planes at some distances away from the discontinuity. The resultant structure is shown in Fig. 1 along with the dimensions and the coordinate system.

As long as the frequency is such that only dominant modes can propagate in the two finline sections and the higher order modes excited at the discontinuity have

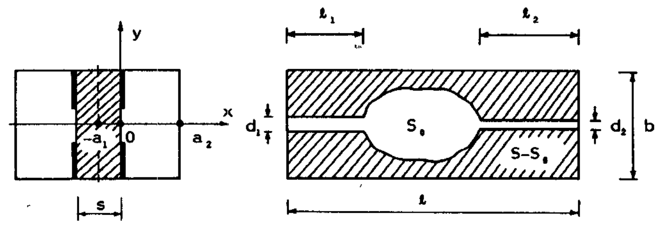

Fig. 1. Transverse and longitudinal cross sections of a finline discontinuity in a shorted cavity.

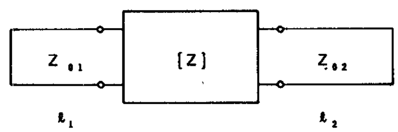

Fig. 2. Equivalent circuit of Fig. 1.

negligible amplitudes at the shorting planes, the discontinuity can be modeled as an equivalent two-port network, as shown in Fig. 2.

The resonance condition in terms of the impedance parameters of the discontinuity is

$$(Z_{11}+Z_1)(Z_{22}+Z_2)-Z_{12}^2=0 \tag{1}$$

where

$$Z_i = jZ_{oi}\tan(\beta_i l_i), \qquad i=1,2.$$

Z_{oi} is the characteristic impedance of the ith finline, and β_i is the corresponding phase constant. Alternatively, (1) can also be formulated in terms of the scattering parameters of the discontinuity.

If the same resonant frequency ω_r rad/s is obtained for three different pairs of l_1, l_2, (1) allows the evaluation of the three impedance parameters of the discontinuity at ω_r.

In the absence of the discontinuity, $\beta_1=\beta_2=\beta$, (1) then reduces to

$$\beta(\omega_r)=n\pi/l$$

with $l=l_1+l_2$. Thus, the length l corresponding to the resonant frequency ω_r yields the phase constant of a uniform finline at ω_r.

With simple modifications, the above procedure can be applied to other types of finline discontinuity problems, such as end effects in open- or short-circuited finline sections. In such cases, the equivalent circuit will consist of a line section terminated at one end with an unknown reactance. Its value can be computed by way of the resonant frequencies of a resonator obtained by short-circuit-

Manuscript received April, 26 1984; revised July 31, 1984. This work was supported in part by the U.S. Army Research Office under Contract DAAG 29-81-K-0053, and in part by the Joint Services Electronics Program.

R. Sorrentino is with the Department of Electronics, University of Rome La Sapienza, Via Eudossiana 18, 00184 Rome, Italy.

T. Itoh is with the Department of Electrical Engineering, University of Texas at Austin, Austin, TX 78712.

0018-9480/84/1200-1633$01.00 ©1984 IEEE

ing the waveguide at some distance away from the line termination.

III. Computation of the Resonant Frequencies

The method for computing the resonant frequencies of the structure will be illustrated in the case of bilateral finline, shown in Fig. 1. The metallic fins are assumed to be infinitely thin, although the method can easily be modified to account the finite thickness of metallization.

Because of symmetry, a longitudinal magnetic plane can be inserted at the symmetric plane $x = -a_1$, so that only the region $x \geqslant -a_1$ has to be analyzed. The extension to nonsymmetrical structures, such as unilateral finlines, is straightforward and will not be considered here.

The EM field in the dielectric region (region 1: $-a_1 \leqslant x \leqslant 0$) and in the air region (region 2: $0 \leqslant x \leqslant a_2$) can be expanded in terms of TE and TM modes of a rectangular waveguide with inner dimensions l and b. We obtain the following expressions for the transverse E- and H-field components in the two regions:

Dielectric Region: $-a_1 \leqslant x \leqslant 0$

$$\boldsymbol{E}_{t1} = \sum_{mn} A'_{mn} \cos k'_{mn}(x+a_1)\hat{\boldsymbol{x}} \times \nabla_t \psi_{mn} + \frac{1}{j\omega\epsilon_0\epsilon_r} \sum_{mn} B'_{mn} k'_{mn} \cos k'_{mn}(x+a_1) \nabla_t \varphi_{mn}$$

$$\boldsymbol{H}_{t1} = \frac{-1}{j\omega\mu_0} \sum_{mn} A'_{mn} k'_{mn} \sin k'_{mn}(x+a_1) \nabla_t \psi_{mn} + \sum_{mn} B'_{mn} \sin k'_{mn}(x+a_1) \nabla_t \varphi_{mn} \times \hat{\boldsymbol{x}}. \quad (2)$$

Air Region: $0 \leqslant x \leqslant a_2$

$$\boldsymbol{E}_{t2} = \sum_{mn} A_{mn} \sin k_{mn}(x-a_2)\hat{\boldsymbol{x}} \times \nabla_t \psi_{mn} - \frac{1}{j\omega\epsilon_0} \sum_{mn} B_{mn} k_{mn} \sin k_{mn}(x-a_2) \nabla_t \varphi_{mn}$$

$$\boldsymbol{H}_{t2} = \frac{1}{j\omega\mu_0} \sum_{mn} A_{mn} k_{mn} \cos k_{mn}(x-a_2) \nabla_t \psi_{mn} + \sum_{mn} B_{mn} \cos k_{mn}(x-a_2) \nabla_t \varphi_{mn} \times \hat{\boldsymbol{x}} \quad (3)$$

where

$$\psi_{mn} = P_{mn} \cos\frac{m\pi z}{l} \cos\frac{n\pi y}{b}$$

$$\varphi_{mn} = P_{mn} \sin\frac{m\pi z}{l} \sin\frac{n\pi y}{b}$$

$$P_{mn} = \sqrt{\frac{\delta_m \delta_n}{lb}} \frac{1}{\gamma_{mn}} \qquad \delta_i = \begin{cases} 1, & i = 0 \\ 2, & i \neq 0 \end{cases}$$

$$\gamma_{mn}^2 = \left(\frac{m\pi}{l}\right)^2 + \left(\frac{n\pi}{b}\right)^2$$

$$k_{mn}^2 = k_0^2 - \gamma_{mn}^2 \qquad k'^2_{mn} = k_0^2 \epsilon_r - \gamma_{mn}^2$$

$$k_0^2 = \omega^2 \mu_0 \epsilon_0 \quad (4)$$

where ψ_{mn} and φ_{mn} are the TE and TM scalar potentials, and m and n are integers with starting values of 0 or 1, depending on whether the TE or TM mode is being considered. P_{mn} are determined from the normalization conditions for ψ_{mn}, φ_{mn}

$$\int_S |\nabla_t \psi_{mn}|^2 \, dS = 1$$

$$\int_S |\nabla_t \varphi_{mn}|^2 \, dS = 1.$$

Equations (2)–(4) already satisfy the boundary conditions at $x = -a_1$ and $x = a_2$. The boundary conditions at $x = 0$ are

$$\boldsymbol{E}_{t1} = \boldsymbol{E}_{t2} = \begin{cases} \boldsymbol{E}_{t0}, & \text{on } S_0 \\ 0, & \text{on } S - S_0 \end{cases} \quad (5)$$

$$\boldsymbol{H}_{t1} = \boldsymbol{H}_{t2} = \boldsymbol{H}_{t0}, \qquad \text{on } S_0 \quad (6)$$

where $\boldsymbol{E}_{to}$ and $\boldsymbol{H}_{to}$ are unknown functions of z, y. These functions are expanded in terms of a set of orthonormal vector functions $\boldsymbol{e}_\nu$, or $\boldsymbol{h}_\mu$ defined over aperture region S_o (see Appendix)

$$\boldsymbol{E}_{to} = \sum_\nu V_\nu \boldsymbol{e}_\nu \quad (7)$$

$$\boldsymbol{H}_{to} = \sum_\mu I_\mu \boldsymbol{h}_\mu. \quad (8)$$

Inserting (2), (3), (7), and (8) into (5) and (6), and making use of the orthogonal properties of $\psi_{mn}, \varphi_{mn}, \boldsymbol{e}_\nu$, and $\boldsymbol{h}_\mu$, we obtain a homogeneous system of equations in terms of unknown coefficients V_ν

$$\sum_\nu V_\nu \left[\xi_{mn\nu} \zeta_{mn\mu} \left(k'_{mn} \tan k'_{mn} a_1 - k_{mn} \operatorname{cotan} k_{mn} a_2 \right) + \chi_{mn\nu} \theta_{mn\mu} k_0^2 \left(\epsilon_r \frac{\tan k'_{mn} a_1}{k'_{mn}} - \frac{\operatorname{cotan} k_{mn} a_2}{k_{mn}} \right) \right] = 0, \qquad \mu = 1, 2 \cdots \quad (9)$$

where

$$\xi_{mn\nu} = \int_{S_0} \hat{\boldsymbol{x}} \times \nabla_t \psi_{mn} \cdot \boldsymbol{e}_\nu \, dS \qquad \chi_{mn\nu} = \int_{S_0} \nabla_t \varphi_{mn} \cdot \boldsymbol{e}_\nu \, dS$$

$$\zeta_{mn\mu} = \int_{S_0} \nabla_t \psi_{mn} \cdot \boldsymbol{h}_\mu \, dS \qquad \theta_{mn\mu} = \int_{S_0} \nabla_t \varphi_{mn} \times \hat{\boldsymbol{x}} \cdot \boldsymbol{h}_\mu \, dS. \quad (10)$$

The condition for nontrival solutions determines the characteristic equation of the given structure. This equation may be regarded as a real function of ω, l_1, and l_2 equated to zero

$$f(\omega, l_1, l_2) = 0. \quad (11)$$

For a given value of $\omega = \omega_r$, (11) can be solved to evaluate three different pairs of l_1 and l_2 yielding the same resonant frequency ω_r. These values of l_1 and l_2 can be used for computing the discontinuity parameters discussed in the previous section.

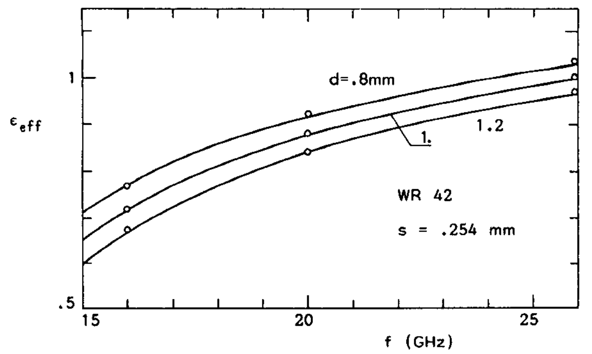

Fig. 3. Effective permittivity of a uniform finline. ∘ Spectral-domain method.

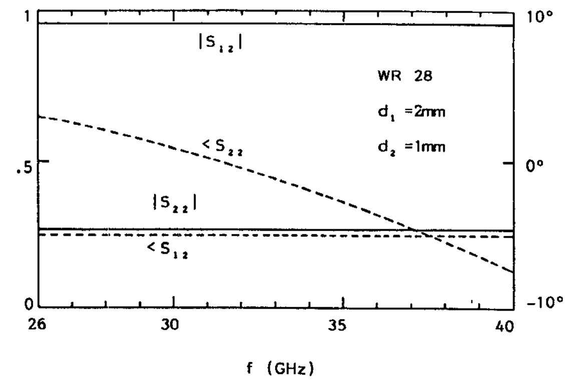

Fig. 5. Scattering parameters of the step discontinuity of Fig. 4.

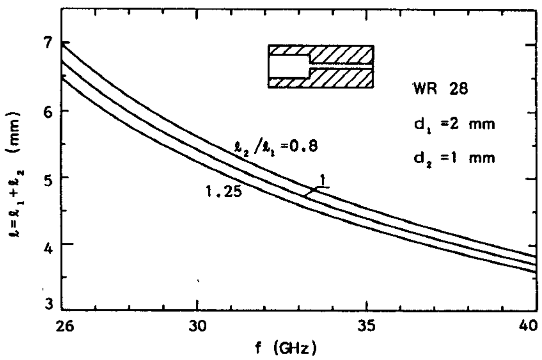

Fig. 4. Resonant frequency of a step discontinuity in a shorted cavity.

IV. Computed Results

According to the above-described technique, the EM fields in the air region, in the dielectric region, and in the aperture region of the resonator are expressed in terms of the series expansions (2), (3), (7), and (8). In the numerical computations, only a finite number of terms of each series can be retained. In order to obtain a proper convergent behavior of the solution, the number of terms in adjacent regions was chosen in such a way that the highest spatial frequencies of the EM field were about the same in the two regions [5], [6]. The method was first tested for computing the propagation characteristics of a uniform finline. In the absence of the discontinuity, the vector basis functions $\boldsymbol{e}_\nu$ and $\boldsymbol{h}_\mu$ on the aperature region (see Appendix) simply reduce to the transverse components of the normal modes of a rectangular waveguide with inner dimensions l and b.

The computed frequency behavior of the effective permittivity

$$\epsilon_{\text{eff}} = (\beta/\beta_0)^2$$

for different gap widths is shown in Fig. 3. Increasing the number of basis functions from 1 to 10, only small differences (less than 1 percent) have been obtained. The time required for computing one resonant frequency using four basis functions was typically 0.3 s on a Univac 1100 computer. The comparison with the results obtained using the spectral-domain approach is quite satisfactory.

In the presence of a step discontinuity, the vector basis functions $\boldsymbol{e}_\nu$ and $\boldsymbol{h}_\mu$ required to represent the EM field over the aperture, have a more complicated spatial distribution, and were evaluated as shown in Appendix. This required some additional computer time.

Fig. 4 shows the resonant frequency of the finline resonator containing a step discontinuity as a function of the total length $l = l_1 + l_2$, with the ratio l_2/l_1 as a parameter. Utilizing these data, the scattering parameters of the discontinuity have been computed using the procedure outlined in Section II, and are shown in Fig. 5. The computed scattering parameters of a unilateral finline discontinuity are compared in Fig. 6 with those computed by Schmidt [5] using the mode-matching procedure.

Although the procedure described above applies to a more complicated discontinuity structure, a certain simplification can be introduced if the discontinuity is longitudinally symmetric, such as the cascaded step discontinuities shown in Fig. 7. For instance, because of the symmetry, the analysis of the structure in Fig. 7(a) is reduced to the two equivalent structures containing a single step terminated by either a magnetic wall or an electric wall, as shown in Fig. 8. The equivalent circuits of the original and the two reduced structures are also shown there.

With obvious modifications of expressions (4) for ψ_{mn} and φ_{mn}, and of the basis functions $\boldsymbol{e}_\nu$ and $\boldsymbol{h}_\mu$ (see Appendix), the field analysis procedure described in Section III can be applied to the case of magnetic walls to obtain Z_{11}, Z_{22}, and Z_{21} by way of the resonant frequencies.

Fig. 9 shows the computed results at 26 GHz for the capacitive strips. The normalized reactance parameters of the equivalent T-network are shown as a function of the fin gap d_2 and the distance h. As expected, the capacitance associated with the shunt branch X_{12} increases with both h and the ratio d_1/d_2. On the contrary, the series branches have an inductive reactance whose value is much less sensitive to variations with respect to d_1/d_2. It can be shown that increasing h or d_1/d_2 results in an increase in the magnitudes of the reflection coefficient s_{11}. The phase of s_{11} varies almost linearly with h.

The dual case of inductive notches is shown in Fig. 10, where the normalized admittance parameters of the equivalent π-network are shown as functions of h and d_2/d_1. In this case, the inductance associated with the series branch

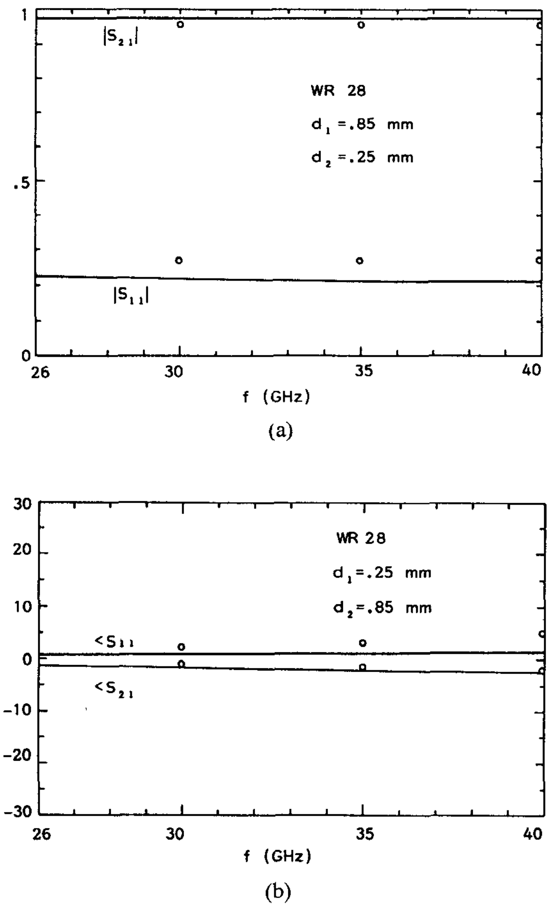

Fig. 6. Scattering parameters of a unilateral finline step discontinuity. ∘ Schmidt [7].

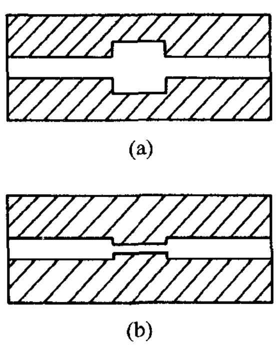

Fig. 7. Cascaded step discontinuities: (a) inductive notch and (b) capacitive strip.

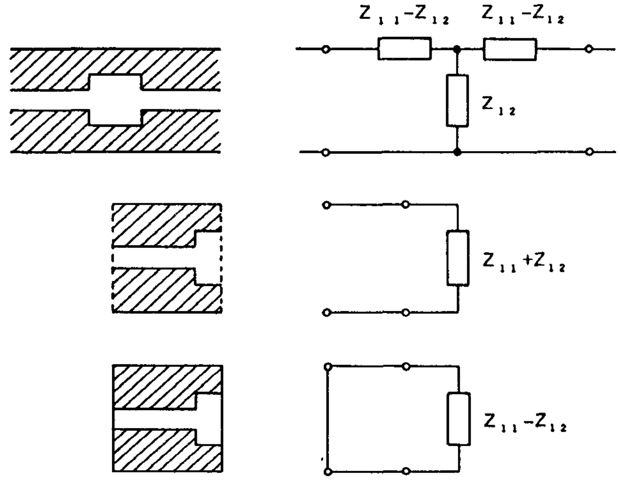

Fig. 8. Evaluation of the Z-parameters of a longitudinally symmetric discontinuity.

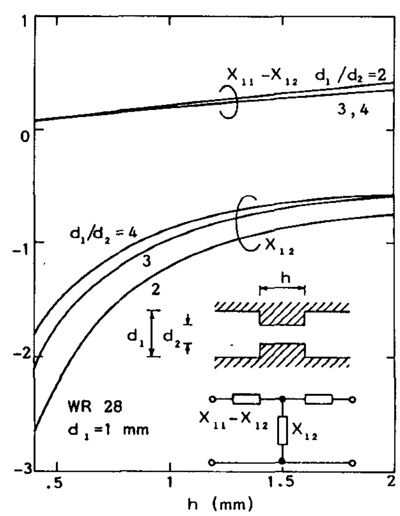

Fig. 9. Normalized reactance parameters of capacitive strips.

increases with h and d_2/d_1, while the capacitance of the shunt branches increases only slightly as a function of these parameters.

V. Conclusions

A new method of analysis has been proposed for the characterization of uniform finlines and finline discontinuities. The method is based on the computation of the resonant frequencies of a resonator obtained by short- (or open-) circuiting a finline section containing the discontinuity. The analysis procedure consists of a field expansion in terms of LSM and LSE modes of the rectangular waveguide. These expressions are matched with the field distribution in the plane of the fins. With respect to other approaches based on the field expansion in terms of finline modes, this procedure reduces computer time. The results are in good agreement with the numerical values obtained with other techniques.

Appendix

The two sets of orthonormalized vector functions $\boldsymbol{e}_\nu$, $\boldsymbol{h}_\mu$ used in (7) and (8) for expanding the EM field at $x=0$ in the aperture region are derived in this Appendix in the case of a step discontinuity between two finline sections of different slot widths. Because of symmetry considerations, a longitudinal electric plane can be placed at $y=0$ (see Fig. 1), so reducing the longitudinal section to that of Fig. 11.

The aperture region $S_0 \equiv (S_1 \cup S_2)$ may be viewed as the cross section of a waveguide having a stepped cross section. We can therefore expand the EM-field components $\boldsymbol{E}_{t0}$, $\boldsymbol{H}_{t0}$ lying in the yz plane in terms of the TE and TM scalar

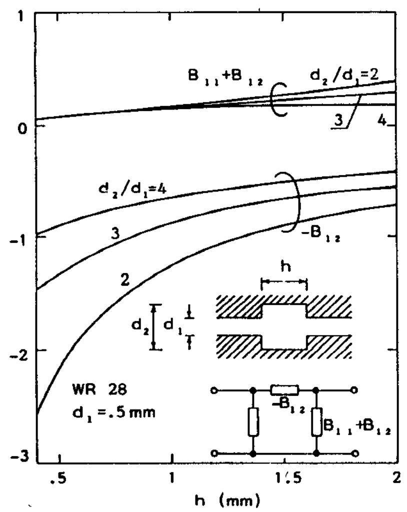

Fig. 10. Normalized admittance parameters of inductive notches.

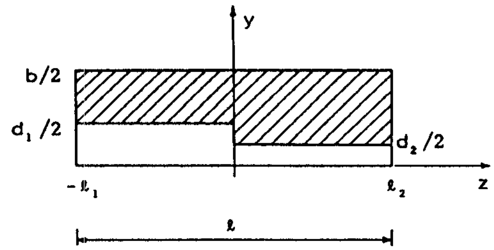

Fig. 11. Reduced geometry of the step discontinuity.

potentials

$$E_{t0}=\sum_n V_n \hat{x}\times\nabla_t\psi_n+\sum_\nu V_\nu\nabla_t\varphi_\nu \tag{A1}$$

$$H_{t0}=\sum_n I_n\nabla_t\psi_n+\sum_\nu I_\nu\nabla_t\varphi_\nu\times\hat{x}. \tag{A2}$$

ψ_n and φ_ν represent the transverse potentials for TE and TM modes, respectively, satisfying the eigenvalue equations

$$\nabla_t^2\psi_n+k_{cn}^2\psi_n=0 \tag{A3}$$

$$\nabla_t^2\varphi_\nu+k_{c\nu}^2\varphi_\nu=0 \tag{A4}$$

in S_0 together with proper boundary conditions.

For the sake of brevity, only the solution of (A3) will be illustrated. Moreover, in order to simplify the notation, the index n will be dropped.

In order to solve (A3), the function ψ can be expressed as follows:

$$\psi=\begin{cases}\psi_1=\sum_r A_r\psi_r^{(1)}, & \text{in } S_1\\ \psi_2=\sum_s B_s\psi_s^{(2)}, & \text{in } S_2\end{cases} \tag{A5}$$

where

$$\psi_r^{(1)}=\cos k_{1r}(z+l_1)\cos\frac{r\pi y}{d_1/2} \tag{A6}$$

$$\psi_s^{(2)}=\cos k_{2S}(z-l_2)\cos\frac{s\pi y}{d_2/2} \tag{A7}$$

$$k_{ir}^2=k_c^2-\left(\frac{r\pi}{d_i/2}\right)^2, \qquad i=1,2. \tag{A8}$$

Expressions (A5)–(A8) are such that (A3) is satisfied together with the boundary conditions at $z=-l_1, l_2$ and $y=0, d_1/2, d_2/2$. The boundary conditions at $z=0$

$$\psi_1=\psi_2, \qquad 0\leqslant y\leqslant d_2/2 \tag{A9}$$

$$\frac{\partial\psi_1}{\partial z}=\begin{cases}\dfrac{\partial\psi_2}{\partial z}, & 0\leqslant y\leqslant d_2/2\\ 0, & d_2/2\leqslant y\leqslant d_1/2\end{cases} \tag{A10}$$

through the orthogonal properties of cosine functions, lead to a homogeneous system of equations in the expansion coefficients A_r, B_s

$$\sum_r A_r f_{rs}\cos k_{1r}l_1-\frac{d_2}{2\delta_s}B_s\cos k_{2s}l_z=0, \qquad s=0,1,2\cdots \tag{A11}$$

$$\frac{d_1}{2\delta_r}A_r k_{1r}\sin k_{1r}l_1+\sum_s B_s f_{rs}k_{2s}\sin k_{2s}l_2=0, \qquad r=0,1,2\cdots \tag{A12}$$

where

$$\delta_r=\begin{cases}1, & r=0\\ 2, & r\neq 0\end{cases}$$

$$f_{rs}=\int_0^{d_2/2}\cos\frac{r\pi y}{d_1/2}\cos\frac{s\pi y}{d_2/2}\,dy.$$

The condition for nontrivial solutions of (A11)–(A12) constitutes the characteristic equation from which the eigenvalues k_c^2 can be computed. For each k_c^2, the expansion coefficients A_r, B_s are determined using (A11)–(A12) and imposing the normalization condition

$$\int_{S_0}|\nabla_\epsilon\psi|^2\,dS=1.$$

Finally, it can be easily demonstrated that the ψ_n's so obtained satisfy the orthogonality condition

$$\int_{S_0}\nabla_\epsilon\psi_n\cdot\nabla_\epsilon\psi_m\,dS=0, \qquad n\neq m$$

even if, for numerical reasons, the series in (A5) will be truncated to a finite number of terms.

A similar procedure can be applied to the evaluation of the φ_ν's. The right-hand side of (A1) and (A2) finally provide the required expansions in terms of orthonormal vector functions.

If the resonator is terminated at $z=-l_1, l_2$ by magnetic walls, (A6) and (A7) are modified corresponding, in order to satisfy the open-circuit boundary conditions. Moreover, the eigenfunction φ_0, corresponding to the eigenvalue $k_c^2=0$, must also be included in expansions (A1) and (A2). This eigenfunction corresponds to the TEM mode of the stepped waveguide with mixed conducting and magnetic boundaries.

References

[1] H. Hofmann, "Dispersion of planar waveguides for millimeter-wave application," *Arch. Elek. Übertragung.*, vol. 31, pp. 40–44, Jan. 1977.

[2] L.-P. Schmidt and T. Itoh, "Spectral domain analysis of dominant and higher order modes in fin-lines," *IEEE Trans. Microwave Theory Tech.* vol. MTT-28, pp. 981–985, Sept. 1980.

[3] A. Beyer, "Calculation of discontinuities in grounded finlines taking into account the metallization thickness and the influence of the mount-slits," in *Proc. of the 12th European Microwave Conf.* (Helsinki, Finland), 1982, pp. 681–686.

[4] H. El Hennaway and K. Schunemann, "Analysis of fin-line discontinuities," in *Proc. of the 9th European Microwave Conf.* (Brighton, England), 1979, pp. 448–452.

[5] S. W. Lee, W. R. Jones, and J. J. Campbell, "Convergence of numerical solutions of iris-type discontinuity problems," *IEEE Trans. Microwave Theory Tech.*, vol. MTT-19, pp. 528–536, June 1971.

[6] Y. C. Shih and K. G. Gray, "Convergence of numerical solutions of step-type waveguide discontinuity problems by modal analysis," in *IEEE MTT-S Int. Symp. Dig.* (Boston, MA), 1983, pp. 233–235.

[7] L.-P. Schmidt, private communication.

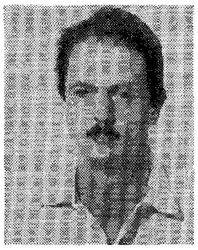

Roberto Sorrentino received a degree in electronic engineering from the University of Rome La Sapienza, Rome, Italy, in 1971.

He then joined the Institute of Electronics of the same University under a fellowship of the Italian Ministry of Education. Since 1974, he has been an Assistant Professor of Microwaves at Rome University La Sapienza. He was also professore incaricato of Microwaves at the University of Catania, Catania, Italy, from 1975 to 1976, and of the University of Ancona, Ancona, Italy, from 1976 to 1977. From 1977 to 1981, he was professore incaricato of Solid State Electronics at the University of Rome La Sapienza, where he is presently an Associate Professor of Microwave Measurements. From September to December 1983, he was appointed as a Research Fellow in the Electrical Engineering Department of the University of Texas at Austin, Austin, TX. His research activities have been concerned with electromagnetic wave propagation in anisotropic media, numerical solution of electromagnetic structures, electromagnetic field interaction with biological tissues, and mainly with the analysis and design of microwave and millimeter-wave integrated circuits.

Since 1978, Dr. Sorrentino has been a member of the Executive Committee of the IEEE Middle and South Italy Section, and is the Chairman of the local MTT Chapter. He is also a member of the Italian Electrical Society (AEI).

Tatsuo Itoh (S'69–M'69–SM'74–F'82) received the Ph.D. degree in electrical engineering from the University of Illinois, Urbana, in 1969.

From September 1966 to April 1976, he was with the Electrical Engineering Department, University of Illinois. From April 1976 to August 1977, he was a Senior Research Engineer in the Radio Physics Laboratory, SRI International, Menlo Park, CA. From August 1977 to June 1978, he was an Associate Professor at the University of Kentucky, Lexington. In July 1978, he joined the faculty at the University of Texas at Austin, where he is now a Professor of Electrical Engineering. During the summer 1979, he was a Guest Researcher at AEG-Telefunken, Ulm, West Germany. Since September 1983, he has held the Hayden Head Centennial Professorship of Engineering at the University of Texas.

Prof. Itoh is a member of the Institute of Electronics and Communication Engineers of Japan, Sigma Xi, and Commissions B of USNC/URSI. He serves on the Administrative Committee of IEEE Microwave Theory and Techniques Society and is the Editor of IEEE TRANSACTIONS ON MICROWAVE THEORY AND TECHNIQUES. He is a Professional Engineer registered in the State of Texas.

Synthesis of Optimum Finline Tapers Using Dispersion Formulas for Arbitrary Slot Widths and Locations

CHRISTIAN SCHIEBLICH, JERZY K. PIOTROWSKI, AND J. H. HINKEN, SENIOR MEMBER, IEEE

***Abstract*—The theory of TEM matching sections has been modified so that it can be applied to finline tapers. A step-by-step procedure is given to calculate the taper contour for a given maximum VSWR. The taper is optimum in the sense that its length is the shortest possible for the required VSWR. To achieve fast convergence, a transversal resonance method was developed to calculate finline dispersion, which is valid for arbitrary slot widths and slot locations. The finline can be unilateral as well as bilateral, and the slot may be off-centered. The dispersion data are compared with values found in the literature, and the calculated taper performance with the authors' own measurements, both showing good agreement.**

Manuscript received April 25, 1984; revised July 27, 1984. This work was supported in part by the Deutsche Forschungsgemeinschaft (DFG) and the German Academic Exchange Service (DAAD).

C. Schieblich is with the Technische Universität Hamburg-Harburg, Arbeitsbereich Elektrotechnik III, Hochfrequenztechnik, Wallgraben 55, D-2100 Hamburg 90, West Germany.

J. K. Piotrowski is with the Institute of Electron Technology, Warsaw Technical University, Koszykowa 75, Warsaw, Poland.

J. H. Hinken is with the Physikalisch-Technische Bundesanstalt, Postfach 3345, D-3300 Braunschweig, West Germany.

I. Introduction

FINLINE COMPONENTS have attracted much attention due to their favorable properties, such as broad single-mode bandwidth, moderate attenuation, sim-

0018-9480/84/1200-1638$01.00 ©1984 IEEE